The Role of Speciation in Alkaline Igneous Fluids During Fenite Metasomatism

D.C. Rubie and W.D. Gunter*
Departement für Erdwissenschaften, ETH-Zentrum, CH-8092 Zürich, Switzerland

Abstract. Fenites associated with alkaline igneous rocks show a progression from a high temperature assemblage consisting of sodium-rich alkali feldspar + a sodium-iron-rich mafic mineral, to an extreme end member assemblage consisting of pure potassium feldspar + iron oxide. The latter assemblage is only found in association with low temperature carbonatites. Segments of this distribution trend can be found in the contact aureole of single intrusive centers.

In the east African Kisingiri nephelinite volcano, ijolite intruded a granodioritic basement, producing a fenitized contact aureole. During metasomatism of granodiorite, according to the mass balance model of Rubie (1982), feldspar only participated in an alkali exchange reaction, while quartz was replaced by sodic pyroxene. Outward from the intrusive contact, with decreasing temperature, feldspar became progressively K-enriched, while pyroxene was enriched in the acmite component. It is predicted that alkali-exchange reactions were controlled by $NaCl^0 - KCl^0$ aqueous complexes close to the intrusive contact, while further out in the aureole $Na^+ - K^+$ ions dominated at the lower temperatures and enhanced the level of potassium metasomatism of feldspar. With decreasing temperature in the aureole, the K/Na ratio of the fluid decreased and consequently the activity of acmite increased.

Around carbonatites, where the level of CO_2 in the escaping fluid can be expected to be high, $Na_2CO_3^0 - K_2CO_3^0$ complexes may dominate. Alkali exchange between feldspar and these aqueous species enhances, even further, the stabilization of pure potassium feldspar. Boiling may also play an important role in potassium metasomatism as carbonatites are frequently associated with pyroclastic rocks. Formation of hematite instead of sodic pyroxene may be attributed to low a_{SiO_2}, high $a_{Fe^{3+}}$ and a CO_2-rich fluid.

Important variables which determine the products of alkali metasomatism are shown to be temperature, pressure and CO_2 content of the fluid, as well as the K/Na ratio of the fluid.

Introduction

Fenitization is a process of alkali metasomatism that occurs around intrusions of ijolite, nepheline syenite, carbonatite, and related rock types (Heinrich 1966; Le Bas 1977). The

* *Present address:* O.S.R.D., Alberta Research Council, 11315 87th Ave., Edmonton, Alberta, T6G 2C2, Canada

Offprint requests to: D.C. Rubie

process characteristically involves a loss or replacement of quartz, growth of sodic pyroxene and/or sodic amphibole, and growth or recrystallization of alkali feldspar. The addition of alkalis is important, and one of the main variables of fenitization is the final Na/K ratio of the metasomatic assemblage. Classification schemes for fenites are usually based on this ratio. Because the feldspar phase can range from albite through perthite to K-feldspar, such terms as 'ultrasodic', 'sodipotassic', and 'ultrapotassic' have been introduced (Siemiatkowska and Martin 1975; Vartiainen and Woolley 1976; Woolley 1982). Within such a classification scheme there is a systematic variation in the composition of sodic pyroxene. Aegirine-augite is generally associated with sodium-rich perthite, and aegirine with potassic feldspar or relict feldspar (Sutherland 1969; Rubie 1971; Vartiainen and Woolley 1976; Rubie and Le Bas 1977a). A summary of the main fenite types is given in Fig. 1. This is not interded to be comprehensive and, for example, it excludes albitite found adjacent to some carbonatites (Denaeyer 1966; Le Bas 1981).

Previous workers have usually discussed the relation between fenite types in terms of source of metasomatizing fluids (e.g. ijolite or carbonatite), temperature, and composition and fractionation of the magma or fluid. We follow with a brief summary of these ideas.

Potassic fenite, consisting of K-feldspar and iron oxide, is the only type that is commonly exclusive to one fluid source (Fig. 1). It is only found associated with carbonatite and indeed is probably the most common product of metasomatism around such intrusions (Le Bas 1977, pp 273–275; Le Bas 1981). More sodic fenites are apparently identical whether associated with ijolite or carbonatite (Fig. 1), but are more common around the former. Assuming that carbonatite forms by immiscibility from an ijolitic magma (Freestone and Hamilton 1980), a coexisting supercritical fluid phase, initially in equilibrium with both melt fractions, would be expected to produce comparable metasomatism around both intrusion types. Long after melt separation however, the respective fluids would be expected to have evolved in different directions, depending on fractionation trends in the two types of melt. The development of potassic fenite seems to be the main evidence, presently available, that this may occur.

Various workers have suggested the temperature-dependence of fenite type (Fig. 1). Such proposals have sometimes been based on position in a thermal aureole and on experimental data. Sutherland (1969) and Rubie and Le Bas (1977a) proposed that aegirine forms in a low temperature

Fig. 1. A summary of mineralogical variations in fenites commonly associated with ijolite, nepheline syenite and carbonatite. Potassic fenites are exclusive to carbonatites. Possible relationships between the types, on the basis of temperature and/or evolving fluid, have been previously suggested (see text)

assemblage and aegirine-augite in a high temperature assemblage. Rubie and Le Bas (1977a), Siemiatkowska and Martin (1975) and Rubie (1982) suggested that the feldspar compositions of Fig. 1 are related to temperature, with sodium-rich perthites favoured by high temperature and K-feldspar by low temperature. Also, Heinrich and Moore (1969) have proposed a low-temperature origin for potassic fenite.

The dependence of fenite type on late changes in composition of the fluid or magma is a further possibility. Siemiatkowska and Martin (1975) suggested that sodic pyroxene is absent in potassic fenites due to a late increase in the K/Na ratio in the fluid. More recently, Woolley (1982) concluded that evolution of carbonatite magma by the loss of Na during early fenitization leads to potassic metasomatism.

Finally, spatial and temporal relationships between fenite types have been recognized. Potassic fenites are thought to characterize high structural levels of carbonatite complexes, with sodic types forming at deep levels (Le Bas 1977, p. 275; Woolley 1982). If different fenite types coexist at the same level, sodic fenites were generally early and evolved into later potassic varieties (Woolley 1969; 1982).

Our purpose in this paper is to assess the importance of temperature, pressure, fluid composition, fluid source, and fluid evolution in fenitization. To start, we examine the effect of temperature by considering feldspar-pyroxene-fluid equilibria along a temperature gradient in fenites adjacent to the Sagurume ijolite intrusion at Kisingiri, western Kenya.

The Sagurume Fenites

The Kisingiri nephelinite volcano is situated in the west Kenyan alkaline igneous province (Le Bas 1977). Pre-volcanic intrusions of ijolite, nepheline syenite and carbonatite were emplaced in a Precambrian basement of granodiorite and granite, and are now partly exposed in the deeply eroded core of the volcano (McCall 1958; Rubie and Le Bas 1977a, b; Rubie 1982). The basement was fenitized around the intrusions, and a particularly well developed metasomatic aureole, 450 m wide, occurs around one of the intrusions, the Sagurume ijolite complex. During fenitization at Sagurume, quartz was replaced by sodic pyroxene, oligoclase by albite, and microcline by orthoclase (Rubie 1971). Within 150–200 m of the intrusion, feldspar recrystallized as perthite. Sodic amphibole developed mainly in rocks originally containing hornblende. Four gradational
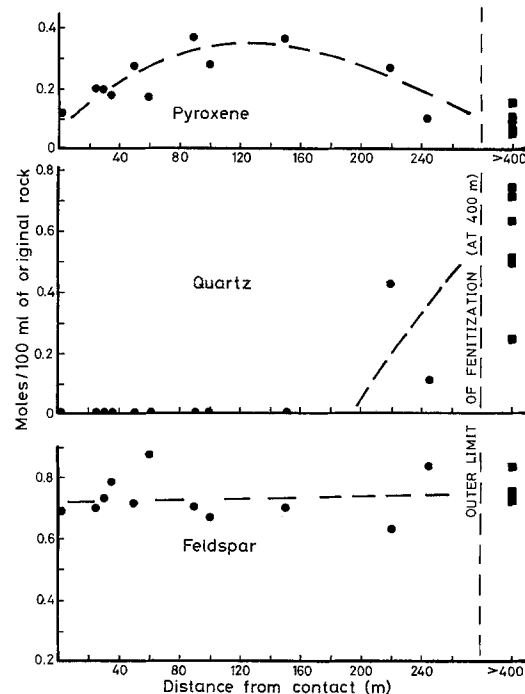

Fig. 2. Molar norms of fenites and unaltered granodiorites calculated from the whole rock analyses of Rubie (1982) in terms of acmite + diopside + hedenbergite, quartz and feldspar, plotted against distance from the intrusive contact. The broken line indicates the approximate trend. See text and Appendix 1 for the method of calculation. In some cases, normative nepheline is present and this has been added to feldspar. Filled circles – fenites, filled squares – granodiorites

zones, concentric to the steep-sided intrusion, have been mapped in fenitized granodiorite (Rubie and Le Bas 1977a; Rubie 1982, Fig. 2). The important features of these zones and their approximate distances from the intrusion margin are:

Zone I (450 m–250 m): Relict quartz and feldspar.
Zone II (250 m–160 m): Relict feldspar, all quartz replaced.
Zone III (160 m–90 m): No relics, mylonitic textures, perthite + aegirine-augite.
Zone IV (90 m–0 m): Recrystallized mylonites, perthite + aegirine-augite; increasingly leucocratic towards the contact.

Small traces of nepheline have been identified in some samples from Zones III and IV (Rubie and Le Bas 1977a). Its occurrence in these zones is by no means ubiquitous, and because its relationships with the other phases are uncertain its presence is not considered in this paper.

The fenites of Zones III and IV are cut by later veins of alkali feldspar + sodic pyroxene (Rubie and Le Bas 1977a), and these are of interest regarding possible fluid and/or temperature evolution.

Mass transfer and volume change during fenitization at Sagurume have been discussed in detail and quantified by Rubie (1982). According to his model, fenitization occurred at approximately constant volume in Zones I–III, but was accompanied by a volume decrease of up to 20% in Zone IV. Aluminum was approximately constant throughout, and feldspars only participated in alkali exchange reactions. Quartz was replaced by sodic pyroxene at constant volume in Zones I–III. Close to the intrusion,

in Zone IV, quartz was removed by dissolution and transport of SiO_2(aq) into the magma, creating a volume reduction and leaving leucocratic rocks enriched in alkali feldspar. On the basis of this model, estimates of elements added and lost, as a function of distance from the intrusion, have been made by Rubie (1982, Fig. 7) using the following definitions derived from Gresens (1967):

Ion content of unaltered rocks, $C_{n,a} = 100 \, \rho_a X_{n,a}/M_n$ (1)

Ion content of altered rocks, $C_{n,b} = 100 \, f_v \rho_b X_{n,b}/M_n$ (2)

where $X_{n,a}$ and $X_{n,b}$ are the weight fractions of element n in the unaltered rock a and in the altered rock b respectively, ρ_a and ρ_b are the respective specific gravities, M_n is the atomic weight of element n, and f_v = final volume/original volume. The units of $C_{n,a}$ and $C_{n,b}$ are moles/100 ml and moles/100 ml of original rock, respectively. In making calculations, it was assumed that the volume change varied linearly from zero at 90 m from the intrusion, to −20% at the contact (Rubie 1982).

We have calculated molar norms of fenite and granodiorite samples in terms of feldspar, quartz and acmite + hedenbergite + diopside components using $C_{n,a}$ and $C_{n,b}$ of Eqs. 1 and 2 and the analyses of Rubie (1982, Table 1). The results of these calculations, plotted against distance from the contact, are presented in Fig. 2, and provide an approximate indication of materials added and subtracted during metasomatism in terms of the above components. The norm calculation, detailed in Appendix 1, gives results comparable with modal compositions for all the fenites except for those rich in amphibole, and these have been omitted (Rubie 1982, Table 1, analyses 6 and 7).

Mineral Chemistry

Electron microprobe analyses of pyroxenes and feldspars have been made using an ARL SEMQ wavelength dispersal system. 15 KV accelerating voltage was used and data were corrected by ZAF procedures.

Representative analyses of sodic pyroxenes from fenites and veins at various distances from the intrusive contact, and from pyroxenite/micro-ijolite at the contact are given in Table 1. Mole fractions of diopside, hedenbergite and acmite, calculated from Mg, Fe^{2+} and Fe^{3+} respectively, form between 92% and 97% of these pyroxenes, and are plotted against distance from the intrusion contact in Fig. 3. In the fenites, pyroxenes become increasingly enriched in acmite with distance from the contact, as previously reported from partial chemical analyses and optical data (Rubie and Le Bas 1977a, Fig. 5.11). The broad spread of analyses in the sample at 245 m (RR1) may be due to a nearby microijolite dyke complicating the history of this rock.

Table 1. Representative microprobe analyses of pyroxenes from fenites and pyroxenite/microijolite at Sagurume

	Fenites							Pyroxenite/Microijolite	
	Zone IV		Zone III		Zone II	Veins			
	RR32	RR16	RR482	RR6	RR1	RR482	RR6	RR39	RR39
Distance:	0 m	30 m	100 m	150 m	245 m	100 m	150 m	(core)	(rim)
SiO_2	51.16	51.74	51.68	52.25	52.04	51.53	50.84	51.17	51.30
TiO_2	0.25	0.30	0.18	0.37	0.59	0.26	0.38	0.67	0.45
Al_2O_3	0.71	1.02	0.55	0.68	1.02	0.84	0.83	1.34	0.96
Fe_2O_3	3.94	4.58	10.17	12.81	12.85	14.29	14.70	3.12	4.53
FeO	11.40	8.80	6.69	7.18	4.20	5.31	10.65	8.19	9.92
MnO	0.59	0.41	0.60	0.56	0.39	0.70	0.59	0.28	0.36
MgO	8.50	9.68	7.68	5.96	7.34	6.17	2.80	11.21	9.32
CaO	21.22	21.03	17.30	14.80	13.99	14.24	13.11	23.02	21.43
Na_2O	1.60	1.98	4.08	5.36	5.61	5.77	6.01	1.21	1.76
K_2O	n.d.	0.01	0.03	0.02	n.d.	n.d.	n.d.	n.d.	0.03
Total	99.37	99.55	98.96	99.99	98.03	99.11	99.91	100.21	100.06
Si	1.973	1.969	1.985	1.998	2.002	1.979	1.985	1.923	1.952
Al^{IV}	0.027	0.031	0.015	0.002	–	0.021	0.015	0.059	0.043
ΣIV	2.000	2.000	2.000	2.000	2.002	2.000	2.000	1.982	1.995
Al^{VI}	0.005	0.015	0.010	0.029	0.046	0.017	0.023	–	–
Ti	0.007	0.009	0.005	0.011	0.017	0.007	0.011	0.019	0.013
Fe^{3+}	0.114	0.131	0.294	0.369	0.372	0.413	0.432	0.088	0.130
Fe^{2+}	0.368	0.280	0.215	0.229	0.135	0.171	0.348	0.258	0.316
Mn	0.019	0.013	0.020	0.018	0.013	0.023	0.020	0.009	0.012
Mg	0.489	0.549	0.440	0.340	0.421	0.354	0.163	0.628	0.529
$\Sigma M1$	1.002	0.997	0.984	0.996	1.004	0.985	0.997	1.002	1.000
Ca	0.887	0.857	0.712	0.606	0.577	0.586	0.548	0.927	0.874
Na	0.120	0.146	0.304	0.397	0.418	0.430	0.455	0.088	0.130
$\Sigma M2$	0.997	1.003	1.016	1.003	0.995	1.016	1.003	1.015	1.004
O	5.992	5.992	5.996	6.009	6.016	5.997	6.004	5.972	5.985

To estimate Fe^{2+} and Fe^{3+}, cations have been calculated to a total of 4, Al^{VI} has been added to Na to form a jadeite component, and Fe has been allocated to the remaining Na as Fe^{3+} to form acmite.

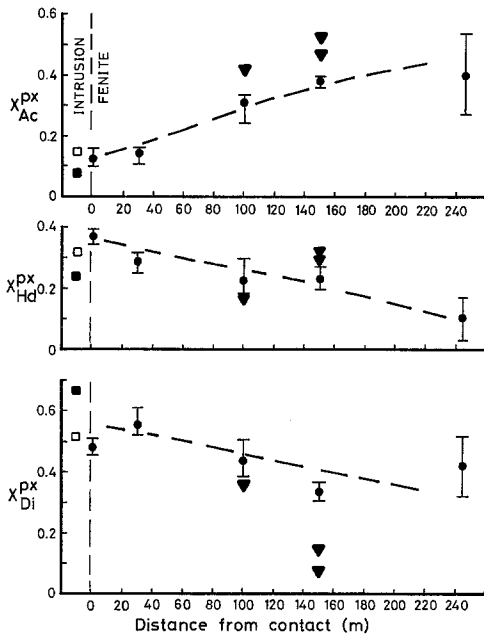Distance = Distance from margin of intrusion in metres. n.d. = not detected

Fig. 3. Pyroxene compositions, calculated as mole fractions of acmite, hedenbergite and diopside, plotted against distance from the intrusive contact. The broken line indicates the approximate trend. Filled circles with bars – average and spread of microprobe analyses of pyroxenes from fenites, filled triangles – vein pyroxenes, closed and open squares – core and rim compositions respectively of pyroxene in pyroxenite/microijolite
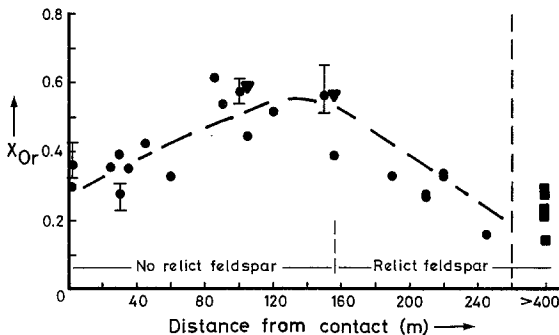

Fig. 4. Feldspar compositions plotted against distance from the intrusive contact. Feldspars are perthites within ~ 180 m of the contact. The broken line indicates the approximate trend. Symbols with bars – average and spread of microprobe analyses (scans), symbols without bars – bulk feldspar separates analysed for Na_2O and K_2O (Rubie 1971); squares – granodiorites, circles – fenites, triangles – fenite veins

Bulk compositional data for feldspars in fenites and granodiorites, obtained from partial analyses of feldspar separates (Rubie 1971) and from electron microprobe scans over perthite and cryptoperthite grains, are plotted as mole fraction of orthoclase component (X_{Or}) against distance from the contact, in Fig. 4. Up to 160 m from the contact, X_{Or} increases with distance from the intrusion. These are compositions that equilibrated during fenitization. Beyond 160 m, relict feldspar becomes increasingly abundant and compositions approach those of the original granodiorite. Overall, there was an enrichment of potassium in the feldspars during fenitization.

Thermal Gradient in the Sagurume Aureole

It is useful to make a semi-quantitative estimate of the temperature gradient in the Sagurume aureole during fenitization for use in subsequent sections on solid-fluid equilibria. Although the following estimates are not very reliable, they do give an indication of relative temperatures. Close to the ijolite contact, the average perthite bulk composition in fenite is $X_{Or} = 0.36$. This allows a minimum temperature of 640–660° C to be estimated from the alkali feldspar solvus (Parsons 1978). Because there is no evidence of melting of the originally granitic rocks at the contact, an upper limit of 770° C is given by the wet granite melting solidus (Tuttle and Bowen 1958), assuming $P_{H_2O} = 500$ bars (based on the height of the pre-volcanic dome at Kisingiri, Le Bas 1977, p. 42). A temperature of $715(\pm 50)°$ C is assumed. Beyond 180 m to 200 m from the contact, alkali feldspar crystallized in the two-phase region. Perthites, of composition $X_{Or} = 0.56$, 150 m from the contact, must have formed close to the solvus, and give a temperature estimate of $610(\pm 20)°$ C (Parsons 1978). For comparison, temperatures of 710° C at the contact, and 620° C at 150 m from the contact have been estimated using heat flow modelling for a syenitic intrusion 1.5 km thick, with a magmatic temperature of 900° C (Jaeger 1957; Winkler 1979).

Fenitization Around Ijolite

Here we consider processes and equilibria to explain the main features of the Sagurume fenites, but which are also applicable to fenitization around ijolites and nepheline syenites in general. Our arguments are based on the following assumptions: (1) Fenitization was caused by a supercritical aqueous CO_2-poor fluid phase, originating from the ijolite magma (Rankin and Le Bas 1973). (2) The principal cation in the fluid was Cl^-. Although Siemiatkowska and Martin (1975) argued against the necessity of Cl^- and proposed complexing of the $Na - Fe^{3+} - OH$ type, Cl^- was certainly present as indicated by analyses of fluid inclusions in alkaline rocks (Sobolev et al. 1974; Le Bas 1981, Table IV). In a following section we also consider the effect of CO_3^{2-} in the fluid. (3) By accepting the volume change model of Rubie (1982), we assume immobile aluminum and therefore constant feldspar (Fig. 2). Whereas such an assumption may be valid for fenitization of granitic rocks, it is certainly not valid when the original rock was quartzite (Deans et al. 1972; Appleyard and Woolley 1979), presumably owing to high gradients in Al activity. (4) We assume that the ratios of activity coefficients $\gamma_{KCl^0}/\gamma_{NaCl^0}$ and $\gamma_{K^+}/\gamma_{Na^+}$ equal unity in an ion pair model (see Appendix 2; Poty et al. 1974, p. 738 and Helgeson et al. 1978, p. 141 for a discussion of activity coefficient bases, activity coefficients and associated errors).

The main features of the Sagurume fenites that we wish to explain are: (1) Removal of quartz from rocks close to the intrusion to give the negative volume change. (2) Replacement of quartz by sodic pyroxene at constant volume beyond ~ 90 m from the intrusion. (3) The increase in the acmite component of pyroxene with distance from the intrusion. (4) The increase in the orthoclase component of feldspar with distance from the intrusion.

We consider reactions between quartz, the components orthoclase, albite and acmite and the aqueous species $NaCl^0$, KCl^0, HCl, H_2O, and SiO_2. We will also include
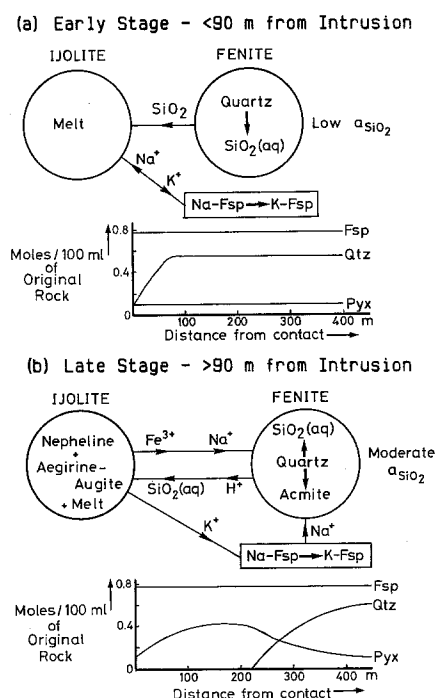
Fig. 5. Mass transfer and reactions during metasomatism around the Sagurume ijolite. Mg, Ca, and Fe^{2+} have been omitted. (a) and (b) relate to stages during the evolution of an a_{SiO_2} gradient. The data of Fig. 2 are schematically reproduced in the molar norm diagram of (b) and the corresponding diagram of (a) depicts an early stage in the evolution of the fenites

the aqueous species Na^+, K^+, $Na_2CO_3^0$ and $K_2CO_3^0$ in following sections. A summary of reactions and mass transfer in fenites close to the contact, and distant from the contact, is given in Figs. 5a and b respectively, and is discussed below. Rocks containing sodic amphibole and biotite are not considered here as they are in a minority at Sagurume and their presence probably depends on bulk composition (Rubie and Le Bas 1977a). In terms of parageneses, this restricts us to two of the six assemblages described in east African fenites by Sutherland (1969).

Pyroxene Stability

The stability of acmite can be described by the reaction

$$2H_2O + Na^+ + Fe^{3+} + 2SiO_2(aq)$$
$$\rightleftharpoons 4H^+ + NaFeSi_2O_6(pyx) \tag{3}$$
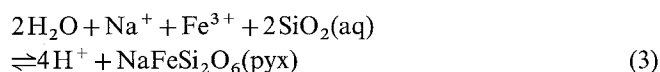
and similar reactions can be written for diopside and hedenbergite components.

The stability of pyroxene can be related to an evolving a_{SiO_2} gradient in the fenites. The activity of silica was presumably buffered in the fenites by two reactions at some stage during their metasomatic evolution:

(1) In rocks containing relict quartz by the reaction

$$SiO_2(Qz) \rightarrow SiO_2(aq). \tag{4}$$

(2) At the fenite-ijolite contact, while nepheline crystallized from the melt, by the equilibrium:

$$NaAlSi_3O_8(Fsp) \rightleftharpoons NaAlSiO_4(Ne) + SiO_2(aq). \tag{5}$$
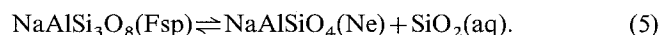
In the early stages of melt fractionation, nepheline was not a stable phase (Rubie and Le Bas 1977a) and presumably a_{SiO_2} at the intrusion margin was buffered by the magma

at a lower value than that defined by reaction (5). A low a_{SiO_2} is expected to have caused the rapid dissolution of quartz and transport of $SiO_2(aq)$ into the magma (Fig. 5a) without pyroxene crystallization by reaction (3). As a result, the fenites close to the contact underwent a volume decrease and became enriched in modal feldspar (Rubie 1982). With increasing distance from the intrusion, a_{SiO_2} must have increased up a gradient towards a value defined by reaction (4); at some point along this gradient pyroxene was stable and crystallized. The formation of acmite by the replacement of quartz at constant volume (Fig. 5b) can be approximately represented by

$$2H_2O + Na^+ + Fe^{3+} + 3SiO_2(Qz)$$
$$\rightarrow 4H^+ + NaFeSi_2O_6(Pyx) + SiO_2(aq). \tag{6}$$
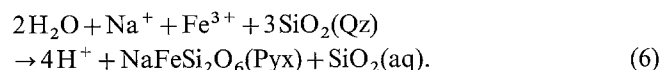
Close to the intrusion margin, a_{SiO_2} in fenites must have increased with time, both due to melt fractionation and due to transport of $SiO_2(aq)$ from the outer parts of the fenite aureole. Consequently pyroxene eventually became stable in these fenites but only crystallized in small modal amounts due to the earlier removal of quartz and the volume decrease.

The sodium content of the fluid increased away from the intrusion due to feldspar-fluid exchange reactions which are described later in detail. The increase in the acmite content of pyroxene, with increasing distance from the intrusion (Fig. 3), is most likely due to this gradient in the fluid composition because, from reactions 3 and 6, the activity of acmite increases as a_{Na^+} increases, provided Fe^{3+} is available. The temperature dependence of the equilibrium constants for reactions 3 and 6 is probably also important, but there are at present no experimental data.

A further factor may be fluid evolution. Pyroxene compositions from pyroxenite and microjolite in the intrusion show an increase in acmite content from core to rim (Table 1; Fig. 3), indicating increasing a_{Na^+} and $a_{Fe^{3+}}$, compared with $a_{Mg^{2+}}$ and $a_{Fe^{2+}}$ during early magma fractionation. A similar trend has been reported in the Napak ijolite by Tyler and King (1967). No systematic zoning has been found in the pyroxenes from Sagurume *fenites,* however.
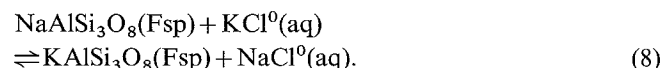
Feldspar-Fluid Equilibria

As shown by Fig. 4, feldspars were affected by a reaction of the type

$$NaAlSi_3O_8(Fsp) + K\text{-complex}(aq)$$
$$\rightarrow KAlSi_3O_8(Fsp) + Na\text{-complex}(aq). \tag{7}$$
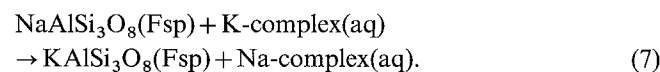
The equilibrium constant for such a reaction is strongly temperature-dependent (Orville 1962, 1963; Lagache and Weisbrod 1977). It has already been suggested that the trend of Fig. 4 is a consequence of the thermal gradient (Rubie 1971; Rubie and Le Bas 1977a; Rubie 1982).

Values of $[KCl^0]/[NaCl^0]$ in an aqueous, CO_2-absent fluid in equilibrium with an alkali feldspar of molar composition X_{Or}, as a function of temperature, have been derived from the data of Lagache and Weisbrod (1977) for the reaction

$$NaAlSi_3O_8(Fsp) + KCl^0(aq)$$
$$\rightleftharpoons KAlSi_3O_8(Fsp) + NaCl^0(aq). \tag{8}$$

The calculations are based on the conclusion that the experimental data of Lagache and Weisbrod (1977) was obtained over a range of conditions at which the associated species
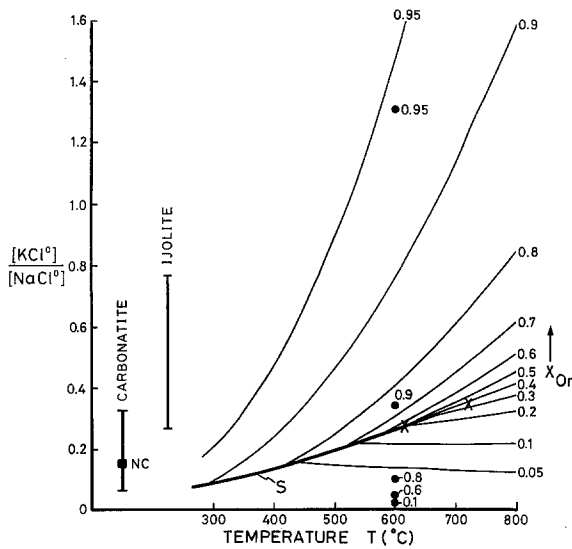
Fig. 6. $[KCl^0]/[NaCl^0]$ for a fluid in equilibrium with alkali feldspar, plotted against temperature (calculated from data of Lagache and Weisbrod 1977), and contoured for feldspar composition (X_{Or}). S, solvus. The bars on the left show the range of fluid inclusion compositions from ijolites and carbonatites reported by Rankin and Le Bas (1973, 1974) and the composition of natrocarbonatite (NC) is also plotted (Dawson 1962; Du Bois et al. 1963). Filled circles show $[K_2CO_3^0]/[Na_2CO_3^0]$ values at 600° C with coexisting X_{Or} values (calculated from data of Iiyama 1965). Crosses: feldspar compositions from Sagurume, plotted at the estimated temperatures of formation

$KCl^0(aq)$ and $NaCl^0(aq)$ predominate over the dissociated species $K^+(aq)$ and $Na^+(aq)$ (see Appendix 2). Values of $[KCl^0]/[NaCl^0]$ are plotted in Fig. 6 for X_{Or} between 0.05 and 0.95, and are independent of pressure at supercritical conditions up to 2 kbar. The range of fluid compositions from fluid inclusions in east African ijolites and carbonatites, reported by Rankin and Le Bas (1973, 1974), are also shown in Fig. 6.

For a fluid of fixed composition, the K-feldspar content of the coexisting feldspar, X_{Or}, generally increases with decreasing temperature. A fluid with $[KCl^0]/[NaCl^0]=0.3$ is in equilibrium with a feldspar of composition $X_{Or}=0.2$ at 700° C and $X_{Or}=0.95$ at 350° C.

Two feldspar compositions from the Sagurume fenites, at 0 m and 150 m from the contact, are plotted on Fig. 6 at their previously estimated temperatures of formation. The corresponding fluid composition for the fenite at 0 m falls within the range of ijolite fluid-inclusion compositions reported by Rankin and Le Bas (1973, 1974). The plots show a compositional gradient in the fluid, with $[KCl^0]/[NaCl^0]$ decreasing away from the intrusion as a result of the exchange reaction with feldspar. Although the temperature estimates have large uncertainties, this gradient must have existed provided that the lower temperature was close to the solvus. The gradient suggests slow-moving fluids with mass transfer predominantly by diffusion, after an initial infiltration stage.

Figure 6 can explain the growth of late-stage albite in fenites adjacent to nepheline syenite intrusions at Kisingiri. The main feldspar is perthite $(X_{Or}=0.54$ or higher) and lower temperatures have been inferred than for the fenites at Sagurume (Rubie and Le Bas 1977a; Rubie 1982). Figure 6 shows that, below 550–600° C, a very small change
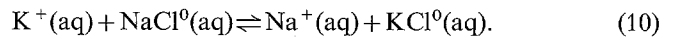
in fluid composition can shift the feldspar composition from high X_{Or}, across the solvus to low X_{Or}. For example, at 500° C, X_{Or} can change from 0.75 to 0.07 with a slight decrease in $[KCl^0]/[NaCl^0]$. A small temperature increase would have a similar effect.

Dissociation of NaCl and KCl

Here we calculate the effect on alkali partitioning if $Na^+(aq)$ and $K^+(aq)$ predominate over $NaCl^0(aq)$ and $KCl^0(aq)$ in the fluid, by the reaction

$$NaAlSi_3O_8(Fsp) + K^+(aq)$$
$$\rightleftharpoons KAlSi_3O_8(Fsp) + Na^+(aq). \tag{9}$$
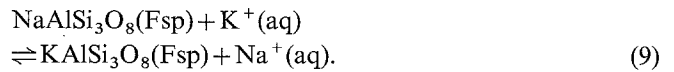
Subtracting Eq. (8) from Eq. (9) gives

$$K^+(aq) + NaCl^0(aq) \rightleftharpoons Na^+(aq) + KCl^0(aq). \tag{10}$$

Because $[K^+]/[Na^+]=[KCl^0]/K_{(10)}[NaCl^0]$, where $K_{(10)}$ is the equilibrium constant for reaction (10), this ratio can be calculated from the values of $[KCl^0]/[NaCl^0]$ of Fig. 6 if $K_{(10)}$ is known. $K_{(10)}=K_{NaCl}/K_{KCl}$, where K_{NaCl} and K_{KCl} are the dissociation constants for NaCl and KCl respectively. We have derived values of $K_{(10)}$ between 300° C and 700° C at $P_{H_2O}=1$ and 2 kbar from the data of Quist and Marshall (1968) for K_{NaCl} and the data of Franck (1956, 1961) and Ritzert and Franck (1968) for K_{KCl}. Values of Log K_{NaCl}, Log K_{KCl} and $K_{(10)}$ are listed in Table 2. Because there are large differences between the K_{KCl} data of Franck (1956, 1961) and Ritzert and Franck (1968), we have calculated two possible sets of $K_{(10)}$ data. According to both sets, $[K^+]/[Na^+]$ is lower than $[KCl^0]/[NaCl^0]$, except at high temperatures ($>600°$ C) at $P_{H_2O}=1$ kbar. The difference is particularly pronounced at low temperature. Much lower values of $[K^+]/[Na^+]$ are predicted by using the K_{KCl} data of Ritzert and Franck (1968) than by using Franck's data. We therefore primarily use the data of Franck and treat the predictions as a limiting case.

In Fig. 7, $[K^+]/[Na^+]$ in the supercritical fluid phase is plotted against temperature for $P_{H_2O}=1$ and 2 kbar, for three values of X_{Or}. P_{H_2O} can be seen to be an important variable, and for a particular fluid composition, with increasing pressure, the coexisting feldspar becomes more potassic. The data therefore show that, under conditions at which the dissociated species predominate, high P_{H_2O} favours potassium metasomatism.

Using the K_{KCl} data of Ritzert and Franck (1968) our conclusions are similar, but the predicted effect of dissociation is more extreme, especially at low temperatures. At 400° C and 2 kbar, the fluid in equilibrium with K-feldspar $(X_{Or}=0.95)$ has the predicted composition $[K^+]/[Na^+]=0.007$, which is an order of magnitude less than the value of Fig. 7.

Gunter and Eugster (1980) and Eugster and Gunter (1981) showed that NaCl and KCl become increasingly dissociated with decreasing temperature, decreasing total molality and increasing P_{H_2O}. The equivalence point for a particular cation is defined by

$$[KCl^0]=[K^+] \quad \text{or} \quad [NaCl^0]=[Na^+].$$

The equivalence point for the dominant cation is easily calculated when its concentration is much greater than that of the other cations. At the equivalence point for NaCl, when $(m_{Na})_{tot}$ is more than 100 times greater than $(m_K)_{tot}$

$$[NaCl^0]=[Na^+] \approx [Cl^-].$$

Table 2a. Dissociation constants K_{NaCl} and K_{KCl} at $P_{H_2O} = 1$ kbar and 2 kbar

	$P_{H_2O} = 1$ kbar					$P_{H_2O} = 2$ kbar				
	300° C	400° C	500° C	600° C	700° C	300° C	400° C	500° C	600° C	700° C
Log K_{NaCl}	0.45[a]	−0.82	−2.12	−3.67	−5.30[a]	0.57[a]	−0.25	−1.07	−1.86	−2.65
Log K_{KCl}(A)	−1.90	−2.15	−2.60	−3.04[a]	−3.49[a]	−1.83	−2.05	−2.25	−2.53	−2.77
Log K_{KCl}(B)	−0.65[a]	−1.25[a]	−2.25	−3.62[a]	−5.10[a]	−0.57[a]	−1.15[a]	−1.70	−2.32	−2.76

K_{NaCl} from Quist and Marshall (1968) − K_{KCl}(A) from Ritzert and Franck (1968) − K_{KCl}(B) from Franck (1956, 1961)

[a] Extrapolated by eye beyond the range of experimental conditions

Table 2b. Values of the equilibrium constant $K_{(10)} = K_{NaCl}/K_{KCl}$ at $P_{H_2O} = 1$ kbar and 2 kbar

	$P_{H_2O} = 1$ kbar					$P_{H_2O} = 2$ kbar				
	300° C	400° C	500° C	600° C	700° C	300° C	400° C	500° C	600° C	700° C
$K_{(10)}$(A)	224	21.4	3.02	0.234	0.0155	251	63.1	15.1	4.68	1.32
$K_{(10)}$(B)	12.6	2.69	1.35	0.891	0.631	13.8	7.94	4.23	2.88	1.29

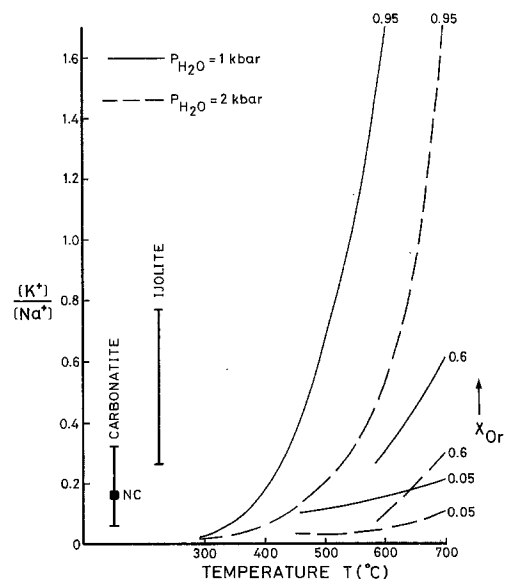**Fig. 7.** $[K^+]/[Na^+]$ for a fluid in equilibrium with alkali feldspar, plotted against temperature for $P_{H_2O} = 1$ and 2 kbar (calculated from data of Lagache and Weisbrod 1977 and the dissociation constants K_{NaCl} and K_{KCl}(B) listed in Table 2a), and contoured for feldspar composition (X_{Or}). Fluid inclusion and natrocarbonatite data are as for Fig. 6

Fig. 8. The dependence of the equivalence points e_{NaCl} and e_{KCl} on total chloride molality $(m_{Cl})_{tot}$ and temperature at $P_{H_2O} = 1$ and 2 kbar (calculated from dissociation constants K_{NaCl} and K_{KCl}(B) listed in Table 2a)

From the total molality equation,

$$(m_{Cl})_{tot} = [NaCl^0] + [Cl^-] + [KCl^0]$$

and

$$(m_{Cl})_{tot} \approx 2 K_{NaCl} \quad \text{(Gunter and Eugster 1980).}$$

We have calculated equivalence points as a function of temperature and total chloride molality at $P_{H_2O} = 1$ and 2 kbar, with both Na and K as the dominant cation (Fig. 8). The tendency for dissociation to increase with pressure is shown in Fig. 8; however this effect becomes less pronounced at low temperatures as shown by the 1 and 2 kbar curves. If Na is the dominant cation, as is probably the case in
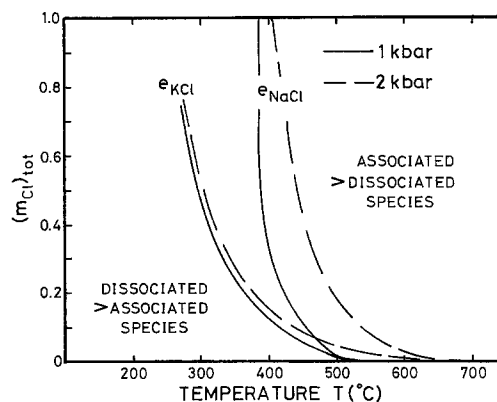
fluids associated with carbonatites and alkaline rocks (Rankin and Le Bas 1974; Sobolev et al. 1974), the dissociated species Na^+ and Cl^- predominate at temperatures below ~400° C. Thus, below 400° C it is more appropriate to use Fig. 7 instead of Fig. 6, when considering partitioning between feldspar and fluid. This leads to the conclusion that K-feldspar is the stable feldspar at low temperatures, except when m_K/m_{Na} in the fluid is extremely low. Above 500° C, dissociation is unlikely to be a contributing factor in feldspar-fluid equilibria.

Veins

Pyroxenes and feldspars have been analyzed in two veins. The feldspar compositions are indistinguishable from those of the host rock (Fig. 4), but the pyroxene is enriched in acmite (Fig. 3, Table 1). A possible interpretation of these data is that the activities of the species in the fluid from which the veins were forming were buffered by the pre-existing feldspar. With decreasing temperature, $[KCl^0]/[NaCl^0]$ then decreases (Fig. 6) and consequently the activity of acmite increases.

Fenitization Around Carbonatite

Fenitization around some carbonatites is little different from fenitization around ijolite and nepheline syenite, and can be described by the reactions of the previous section. However, in many cases the product of metasomatism is potassic fenite, typically consisting of K-feldspar and iron oxide (Fig. 1; Le Bas 1981). We wish to explain the highly potassic nature of the feldspar alteration, and the formation of hematite, either by the breakdown of sodic pyroxene or by direct precipitation.
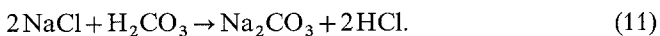
Feldspar-Fluid Equilibria

Potassium metasomatism around carbonatite can be explained by low temperatures, at which there is strong partitioning of Na into the fluid and K into feldspar. According to Fig. 6, K-feldspar with $X_{Or} > 0.9$ is in equilibrium with a fluid equivalent to an average carbonatite fluid inclusion composition at 375° C or below if $NaCl^0(aq)$ and $KCl^0(aq)$ dominate. However, because the dissociated species $(K^+(aq)$ and $Na^+(aq)$ are predicted to be dominant at $T < 400°$ C (Fig. 8), the true equilibrium feldspar may be even more potassic (Fig. 7). An example of low temperature potassium metasomatism is found in Yellowstone Park where oligoclase is being replaced by K-feldspar at 180° C by exchange with thermal waters of composition $m_K/m_{Na} = 0.025$ (White 1955). The high sodium content of carbonatitic fluids, compared with ijolitic fluids (Figs. 6 and 7), could be the result of exchange reactions with feldspar.
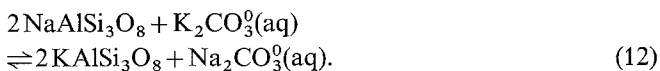
We now consider how the partitioning of Na and K between feldspar and fluid is affected by: (1) CO_2-rich fluids, and (2) boiling.

CO_2-Rich Fluids

Fluid-inclusion data show that fluids associated with crystallizing carbonatites were aqueous and rich in CO_2 (Rankin 1975). The presence of CO_2 in an aqueous fluid introduces Na_2CO_3 and K_2CO_3 species, e.g.:

$$2NaCl + H_2CO_3 \rightarrow Na_2CO_3 + 2HCl. \tag{11}$$

For the reaction

$$2NaAlSi_3O_8 + K_2CO_3^0(aq)$$
$$\rightleftharpoons 2KAlSi_3O_8 + Na_2CO_3^0(aq). \tag{12}$$

$[K_2CO_3^0]/[Na_2CO_3^0]$ can be calculated for X_{Or} values at 600° C, using the experimental data of Iiyama (1965). If there were no carbonate complexes but only charged ions (i.e. K^+, Na^+, CO_3^{2-}, HCO_3^-), we would expect a K_{total}/Na_{total} in the carbonate solution similar to that predicted for the univalent ions of the chloride solutions plotted in Fig. 7. Because this is not the case, we assume that neutral carbonate aqueous complexes dominate at 600° C and 1 kbar, as do neutral chloride ion pairs. (However, this assumption is subject to uncertainties in the dissociation constant data). Subtracting Eq. (8) from Eq. (12) gives

$$K_2CO_3^0 + 2NaCl^0 \rightleftharpoons Na_2CO_3^0 + 2KCl^0. \tag{13}$$
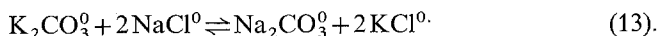
The equilibrium constant for this reaction is given by

$$K_{(13)} = \frac{[Na_2CO_3^0][KCl^0]^2}{[K_2CO_3^0][NaCl^0]^2} = 1.70 \text{ at } 600° \text{ C and 1 kbar}$$

from the data of Iiyama (1965, Table 1). Unfortunately no other data exist to be able to extrapolate $K_{(13)}$ to other

temperatures and pressures. We have calculated $[K_2CO_3^0]/[Na_2CO_3^0]$ for X_{Or} values using previously calculated values of $[KCl^0]/[NaCl^0]$ and the results are plotted, for 600° C, in Fig. 6.

The effect of CO_3^{2-} speciation is to strongly partition Na into the fluid and K into the feldspar, in comparison with Cl^- speciation. A K-rich feldspar $(X_{Or} = 0.85)$ can be in equilibrium with an average carbonatite fluid $(m_K/m_{Na} = 0.2)$ at temperatures as high as 600° C. These data show that large amounts of CO_2 in the fluid phase will promote potassium metasomatism. Conversely, for ijolite fenitization, such as at Sagaurume, fluids must be poor in CO_2. These observations agree with the fluid-inclusion data of Rankin and Le Bas (1973) and Rankin (1975) regarding the respective CO_2 contents of ijolitic and carbonatitic fluids.

The species SO_4^{2-} has a similar effect to CO_3^{2-} (Iiyama 1965). Its presence may also contribute to potassium metasomatism as it is a significant species in fluid inclusions in at least some alkaline rocks (Sobolev et al. 1974).

Boiling

Fournier (1976) has shown that the KNa_{-1} exchange according to reaction (8) is significantly enhanced when the fluid phase unmixes to gas + brine at subcritical pressures, the only exception being when the bulk composition is very rich in potassium. For example, at 600° C and $P_{H_2O} < 180$ bars, the most sodic feldspar to form experimentally was $X_{Or} = 0.83$ in equilibrium with a gas + brine + salt composition of $[KCl]/[NaCl]$ between 0.024 and 0.15. For a supercritical fluid of this composition, Fig. 6 predicts, in contrast, a feldspar composition of $X_{Or} = 0.05$.

Experimental data of Lagache and Weisbrod (1977) show a marked reduction in $[KCl]/[NaCl]$ for low total molalities (< 1 m–2 m). This trend is most apparent at low pressures, depending on temperature, and is undetectable at 1,000 bars. They suggested that, with decreasing pressure and total molality, the fluid composition moves into the two-phase liquid + vapour region in the $NaCl - KCl - H_2O$ system, with a resulting change in partitioning. There is also the possibility that, at low molality, dissociation of NaCl and KCl produces this effect, but because dissociation is favoured by high pressure, boiling is more likely in this case.

Lagache and Weisbrod (1977) discussed high temperature potassium metasomatism by the mechanism of isothermal fluid pressure reduction as a result of the opening of fractures etc. If the pressure reduction is sufficient, the fluid unmixes to a gas + brine, and alkali feldspar is enriched in K relative to its former equilibrium composition. This mechanism is directly applicable to carbonatite metasomatism. Carbonatite emplacement is usually accompanied by widespread fracturing, shattering and brecciation of the basement rocks, and by the formation of both intrusive and extrusive pyroclastic rocks (Heinrich 1966; Tuttle and Gittins 1966; Le Bas 1977). The emplacement of highly potassic trachyte dykes is also characteristic; a fluidization mechanism has been proposed for their emplacement, as well as for some of the intrusive pyroclastics (Sutherland 1965; Rubie 1971; Rubie and Le Bas 1977b; Le Bas 1977). All of these processes are compatible with a rapid reduction in fluid pressure, which is likely to have led to boiling and potassium metasomatism.

Acmite/Hematite Stability

The replacement of acmite by hematite, or the preferential precipitation of hematite, can be represented by:

$$2H^+ + 2NaFeSi_2O_6(cpx)$$
$$\rightarrow Fe_2O_3(hem) + 2Na^+ + 4SiO_2(aq) + H_2O. \tag{14}$$
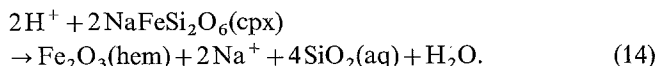
Low a_{SiO_2} would favour hematite precipitation but, because acmite is present in fenites around some carbonatites, this may not be the only factor. Possible contributions to the breakdown of acmite are: (1) High a_{H^+} resulting from high CO_2 content. (2) High $a_{Fe^{3+}}$ leading to hematite saturation. Le Bas (1977) showed that with fractionation, Fe^{3+} becomes increasingly abundant in carbonatites, and presumably this also applies to the associated fluid phase. (3) Low a_{Na^+} as carbonatites become depleted in alkalis. (4) Low temperature should not favour hematite over acmite because hematite and magnetite solubility increase rapidly as temperature is lowered (Chou and Eugster 1977), and under some conditions acmite is stable at room temperature (Milton and Eugster 1959). There are no experimental data on the subsolidus stability of acmite, but presumably with low a_{SiO_2} and high a_{H^+}, acmite may break down at low temperature according to reaction (14).

Conclusions

1) Fenitization around ijolites develops at high temperatures in the presence of a CO_2-poor fluid phase. Important factors in determining the resulting feldspar composition are the m_K/m_{Na} of the fluid, and temperature. At supercritical conditions up to 2 kbar, feldspar-fluid equilibria are independent of fluid pressure at $T>350-400°$ C (Lagache and Weisbrod 1977). With decreasing temperature, K partitions into the feldspar, Na into the fluid, and consequently coexisting pyroxenes become more acmitic.

2) Carbonatite melts, originating by immiscibility from silicate melts, can be assumed to originally have a high alkali content, and their composition is probably close to that of the Oldoinyo Lengai natrocarbonatite (Le Bas 1981). Because intrusive carbonatites have a very low alkali content, alkalis are lost during crystallization via the fluid phase which metasomatizes the surrounding rocks. There is no compelling reason to suppose that Na is lost via the fluid at an early stage and K at a late stage, as proposed by Woolley (1982) to explain different types of metasomatism. The variety of fenite types found around carbonatites can all be formed by a fluid phase of constant m_K/m_{Na}, such as that of the natrocarbonatite. Factors that determine Na$-$K partitioning between feldspar and fluid largely determine the fenite type, and include temperature, pressure, and CO_2 content of the fluid.

3) At high temperatures (e.g. $>650°$ C) adjacent to ijolite and carbonatite, alkali feldspars of intermediate composition can form in equilibrium with a fluid. At moderate to low temperatures, feldspar compositions are either Na-rich or K-rich, due to the presence of the solvus (Fig. 6).

4) Sodium metasomatism, and the formation of albitite adjacent to a carbonatite, is favoured by high temperatures (e.g. $>500°$ C) and a supercritical CO_2-poor aqueous fluid, if the m_K/m_{Na} ratio is typical of carbonatite fluid inclusions.

5) Potassium metasomatism, and the formation of potassic fenite from a fluid with m_K/m_{Na} typical of carbonatite fluid inclusions, is favoured by: (a) Low temperature ($<400-450°$ C) if the supercritical aqueous fluid is poor in CO_2 (Fig. 6). Dissociation of $NaCl^0$ and KCl^0 may make an important contribution to alkali partitioning under these conditions, in which case potassium metasomatism is further enhanced by increasing pressure (Fig. 7). (b) Temperatures of up to 600° C when the supercritical aqueous fluid is rich in CO_2. (c) High temperatures (e.g. 600° C) and a rapid reduction in fluid pressure, such that the fluid boils. In view of the applicability of these factors to metasomatism around carbonatites, it is hardly surprising that potassic fenite is so common.

(6) Spatial and temporal variations in fenitization products can be related to T, P and CO_2 content of the fluid. The development of sodic fenite at deep levels and potassic fenite at shallow levels around an intrusion can be related to temperature gradients in the thermal aureole. Sequences of early sodic fenite evolving into later potassic fenite can be explained by falling temperatures and/or rising levels of CO_2 in the fluid and/or a transition from supercritical to subcritical conditions.

(7) Owing to lack of data on subsolidus acmite stability, we can only hypothesize on the precipitation of hematite in place of sodic pyroxene in potassic fenite. Contributing factors must be low a_{SiO_2}, high $a_{Fe^{3+}}$ and a_{H^+}, and probably low temperature. $a_{Fe^{3+}}$ evidently increases in the fluid with carbonatite fractionation and evolution, and leads at low temperature to hematite saturation.

Appendix 1

Molar Norm Calculation

The whole rock analyses of Rubie (1982, Table 1) were recalculated using Eq. 1 for granodiorite analyses and Eq. 2 for fenite analyses. The following steps were then followed: 1) Acmite, hedenbergite and diopside components equal Fe^{3+}, Fe^{2+} and Mg respectively. 2) Anorthite equals excess Ca remaining after the pyroxene calculation. 3) Total feldspar is calculated from Al and previously calculated anorthite. 4) Quartz equals Si remaining after steps 1–3. 5) If Si is insufficient for steps 1–3, the result of 3 is discarded and feldspar and nepheline are calculated from the Si and Al remaining after (2).

Appendix 2

Ion Pairing

There are a number of different choices for our solution model for the aqueous fluid. Much of the alkali feldspar-fluid exchange literature (Lagache and Weisbrod 1977; Thompson and Waldbaum 1968) uses a stoichiometric model in which the stoichiometric activity coefficients refer to the total concentration of a specific molecule (i.e. sum of free and associated ions) in the fluid. Dissociation constants have been measured for NaCl and KCl (Quist and Marshall 1968; Franck 1956) over the same temperature and pressure range as data exist for the exchange reactions. The dissociation constants can be used for formulating an
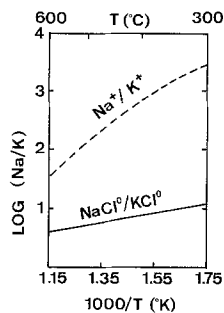
Fig. A-1. Composition of the aqueous fluid in equilibrium with solvus alkali feldspars between 300° C and 600° C at 2 kbar. From Gunter and Eugster (1980, Fig. 11) and data of Quist and Marshall (1968) and Ritzert and Franck (1968)

ion pair model in which the activity coefficients are related to specific free ions (Na^+, K^+) or associated ions ($NaCl^0$, KCl^0). The advantage of using a model of ion pairing is that the activity coefficients (γ_{NaCl^0}, γ_{KCl^0}, γ_{Na^+}, γ_{K^+}) vary in a simpler fashion than in the stoichiometric model in which the coexistence of different aqueous species must be hidden in the activity coefficients ($\gamma_{Na(total)}$, $\gamma_{K(total)}$). We have used the ion pair model in this paper.

The activity coefficients of the neutral ion pairs vary similarly in response to decrease of free solvent water because of take up of H_2O into hydration spheres dominantly forming around charged ions. If the ionic strength of an aqueous solution is low and ion pairs predominate, then $\gamma_{NaCl^0} \approx \gamma_{KCl^0} \approx 1$. On the other hand the activity coefficients of the charged species are much more sensitive to ion-ion interactions and vary strongly at low ionic strengths ($I < 0.5$). Consequently the assumption of ideal mixing of ion pairs can be used safely in $P - T$ regions where neutral ion pairs predominate. Otherwise the ideal behaviour only occurs in dilute solutions.

Unfortunately activity coefficient data only exist at low temperatures but give a maximum estimate of departure from ideality because the aqueous solution tends towards more ideal behaviour with increasing temperature when mixing is based on the ion pair model. Solutions at 25° C with $I < 1.0$ have $\gamma_{K^+,Na^+} > 0.6$ based on the Debye-Hückel and the mean salt methods. Actually the errors contained in our calculations will be lessened because only ratios of activity coefficients are considered. Although γ_{K^+,Na^+} vary from 06. to 1.0, the ratio $\gamma_{K^+}/\gamma_{Na^+}$ only varies from 0.8 to 1 with $I < 1$.

In Fig. A-1, the aqueous solution composition in equilibrium with a solvus alkali feldspar has been plotted over a range of temperatures at a pressure of 2 kbar using the data from Fig. 11 of Gunter and Eugster (1980). Between 300° C and 600° C the ratio of Na^+/K^+ exceeds the $NaCl^0/KCl^0$ ratio by a factor which ranges from 10 to 100. Although this difference may be reduced due to the uncertainty of this data as discussed above, it will still remain significant. If a stoichiometric rather than an ion pair model was used this difference would have to be taken up in $\gamma_{NaCl(total)}/\gamma_{KCl(total)}$ resulting in a large departure from 1 for this ratio, which would rapidly change as the transition point is approached between charged ion dominance and neutral ion pair dominance in the aqueous solution.

Lagache and Weisbrod (1977) have shown from experiments on the alkali feldspar-fluid exchange reaction that, at temperatures from 350° C to 650° C and pressures less

than 2 kbar, $\gamma_{Na(total)}/\gamma_{K(total)}$ is a constant for each specific P and T and is independent of $m_{Cl(total)}$ between 0.5 to 14 molal in alkali chloride aqueous solutions. We interpret these results to mean that the dominant form of species did not change over the concentration range investigated. This conclusion is collaborated in Fig. 8 which shows that, above 400° C and at pressures less than 2 kbar, the dominant forms of the alkali aqueous species are the ion pairs $NaCl^0$ and KCl^0. Consequently $m_{K(total)} \approx m_{KCl^0}$, $m_{Na(total)} \approx m_{NaCl^0}$, and $\gamma_{Na(total)}/\gamma_{K(total)} \approx \gamma_{NaCl^0}/\gamma_{KCl^0}$ over the $P - T$ range of their experiments. For this case large errors will not be introduced by assuming that $\gamma_{NaCl}/\gamma_{KCl}$ is unity.

References

Appleyard EC, Woolley AR (1979) Fenitization: An example of the problems of characterizing mass transfer and volume changes. Chem Geol 26:1–15

Chou I-Ming, Eugster HP (1977) Solubility of magnetite in supercritical chloride solutions. Am J Sci 227:1296–1314

Dawson JB (1962) Sodium carbonate lavas from Oldoinyo Lengai, Tanganyika. Nature 195:1075–1076

Deans T, Sukheswala RN, Sethna SF, Viladkar SG (1972) Metasomatic feldspar rocks (potash fenites) associated with the fluorite deposits and carbonatites of Amba Dongar, Gujarat, India. Inst Mining and Metallurgical Trans (sect B: Appl Earth Sci) 81:B1–B9

Denaeyer ME (1966) Sur la présence d'une carbonatite ankéritique (raughaugite) en boudure du complexe alcalin de Kirumba (Kivu). C.R. Acad Sci Paris 263(D):9–12

Du Bois CGB, Furst J, Guest NJ, Jennings DJ (1963) Fresh natrocarbonatite lava from Oldoinyo L'Engai. Nature 197:445–446

Eugster HP, Gunter WD (1981) The compositions of supercritical metamorphic solutions. Bull Mineral 104:817–826

Fournier RO (1976) Exchange of Na^+ and K^+ between water vapor and feldspar phases at high temperature and low vapor pressure. Geochim Cosmochim Acta 40:1553–1561

Franck EU (1956) Hochverdichteter Wasserdampf III. Ionendissoziation von KCl, KOH und H_2O in überkritischem Wasser. Z Phys Chem 8:192–206

Franck EU (1961) Überkritisches Wasser als elektrolytisches Lösungsmittel. Angew Chem 73:309–322

Freestone IC, Hamilton DL (1980) The role of liquid immiscibility in the genesis of carbonatites – An experimental study. Contrib Mineral Petrol 73:105–117

Gresens RL (1967) Composition-volume relations of metasomatism. Chem Geol 2:47–65

Gunter WD, Eugster HP (1980) Mica-feldspar equilibria in supercritical alkali chloride solutions. Contrib Mineral Petrol 75:235–250

Heinrich EW (1966) The Geology of Carbonatites. Rand McNally, Chicago

Heinrich EW, Moore DG (1969) Metasomatic potash feldspar rocks associated with alkalic igneous complexes. Can Mineral 10:136

Helgeson HC, Delaney JM, Nesbitt HW, Bird DK (1978) Summary and critique of the thermodynamic properties of the rock forming minerals. Am J Sci 278A:1–229

Iiyama JT (1965) Influence des anions sur les équilibres d'échange d'ions Na – K dans les feldspaths alcalines à 600° C sous une pression de 1000 bars. Bull Soc Franc Mineral Crist LXXXVIII:618–622

Jaeger JC (1957) The temperature in the neighbourhood of a cooling intrusive sheet. Am J Sci 255:306–318

Lagache M, Weisbrod A (1977) The system: Two alkali feldspars-KCl – NaCl – H_2O at moderate to high temperatures and pressures. Contrib Mineral Petrol 62:77–101

Le Bas MJ (1977) Carbonatite-Nephelinite Volcanism. J. Wiley & Sons, New York

Le Bas MJ (1981) Carbonatite magmas. Mineral Mag 44:133–140

McCall GJH (1958) Geology of the Gwasi area. Geol Surv Kenya, Rept 45

Milton C, Eugster HP (1959) Mineral assemblages of the Green River Formation. In: Abelson PH (ed) Researches in geochemistry, John Wiley & Sons, New York, pp 118–150

Orville PM (1962) Alkali metasomatism and feldspars. Norsk Geol Tidsskr 42:283–316

Orville PM (1963) Alkali ion exchange between vapor and feldspar phases. Am J Sci 261:201–237

Parsons I (1978) Alkali-feldspars: which solvus? Phys Chem Minerals 2:199–213

Poty PB, Stalder HA, Weisbrod AM (1974) Fluid inclusion studies in quartz from fissures of Western and Central Alps. Schweiz Mineral Petrogr Mitt 54:717–752

Quist AS, Marshall WL (1968) Electrical conductances of aqueous sodium chloride solutions from 0°–800° C and at all pressures to 4,000 bars. J Phys Chem 72:684–703

Rankin AH (1975) Fluid inclusion studies in apatite from carbonatites of the Wasaki area of western Kenya. Lithos 8:123–136

Rankin AH, Le Bas MJ (1973) A study of fluid inclusions in alkaline rocks with special reference to critical phenomena. J Geol Soc Lond 129:319

Rankin AH, Le Bas MJ (1974) Nahcolite (NaHCO$_3$) in inclusions in apatites from some east African ijolites and carbonatites. Mineral Mag 39:564–570

Ritzert G, Franck EU (1968) Elektrische Leitfähigkeit wässeriger Lösungen bei hohen Temperaturen und Drucken. I. KCl, BaCl$_2$, Ba(OH)$_2$, und MgSO$_4$ bis 750° C und 6 kbar. Ber Bunsenges Phys Chem 72:798–808

Rubie DC (1971) The structure and petrology of the Kisingiri nephelinitic volcano, western Kenya. Unpublished Ph.D. thesis, University of Leicester

Rubie DC (1982) Mass transfer and volume change during alkali metasomatism at Kisingiri, western Kenya. Lithos 15:99–109

Rubie DC, Le Bas MJ (1977a) Kisingiri: The sub-volcanic alkali silicate rocks. In: Le Bas MJ, Carbonatite-nephelinite volcanism, John Wiley & Sons, New York, pp 47–79

Rubie DC, Le Bas MJ (1977b) Kisingiri: The early carbonatitic activity. In: Le Bas MJ, Carbonatite-nephelinite volcanism, John Wiley & Sons, New York, pp 80–86

Siemiatkowska KM, Martin RF (1975) Fenitization of Mississagi quartzite, Sudbury area. Geol Soc Amer Bull 86:1109–1122

Sobolev VS, Bazarov TYu, Kostyuk VP (1974) Inclusions in the minerals of some types of alkaline rocks. In: Sorensen H (ed) The alkaline rocks, John Wiley & Sons, New York, pp 389–401

Sutherland DS (1965) Potash-trachytes and ultrapotassic rocks associated with the carbonatite complex of the Toror Hills, Uganda. Mineral Mag 35:363–378

Sutherland DS (1969) Sodic amphiboles and pyroxenes from fenites in east Africa. Contrib Mineral Petrol 24:114–135

Thompson JB, Waldbaum DR (1968) Mixing properties of sanidine crystalline solutions. I: Calculations based on ion-exchange data. Am Mineral 53:1965–1999

Tuttle OF, Bowen NL (1958) Origin of granite in the light of experimental studies in the system $NaAlSi_3O_8 - KAlSi_3O_8 - SiO_2 - H_2O$. Geol Soc Am Mem 74

Tuttle OF, Gittins J (1966) Carbonatites. John Wiley & Sons, New York

Tyler RC, King BC (1967) The pyroxenes of the alkaline igenous complexes of eastern Uganda. Mineral Mag 36:5–21

Vartiainen H, Woolley AR (1976) The petrography, mineralogy and chemistry of the fenites of the Sokli carbonatite intrusion, Finland. Geol Surv Finl Bull 280

White DE (1955) Thermal springs and epithermal ore deposits. Econ Geol, 50th Anniversary Vol:99–154

Winkler HGF (1979) Petrogenesis of metamorphic rocks, 5th ed. Springer, New York

Woolley AR (1969) Some aspects of fenitization with particular reference to Chilwa Island and Kangankunde, Malawi. Bull British Museum (Nat Hist) Mineral 2:189–219

Woolley AR (1982) A discussion of carbonatite evolution and nomenclature, and the generation of sodic and potassic fenites. Mineral Mag 46:13–17